ELSEVIER

Journal of Nuclear Materials 307–311 (2002) 1600–1608

journal of nuclear materials

www.elsevier.com/locate/jnucmat

Section 15. Small specimen technology

Recent progress in small specimen test technology

G.E. Lucas [a,*], G.R. Odette [a], M. Sokolov [b], P. Spätig [c], T. Yamamoto [a], P. Jung [d]

[a] *Department of Mechanical and Environmental Engineering, UC Santa Barbara, Santa Barbara, CA 93106, USA*
[b] *Oak Ridge National Laboratory, P.O. Box 2008, Oak Ridge, TN 37831, USA*
[c] *EPFL/CRPP, Fusion Technology Materials, OVGA/2, CH-5232 Villigen PSI, Switzerland*
[d] *Institut für Festkörperforschung, Forschungszentrum, D-52425 Jülich, Germany*

Abstract

Small specimen test technology (SSTT) has enabled the development of fusion materials by efficiently using available irradiation volumes. The technology has also evolved in anticipation of the construction and operation of a high-energy neutron source for development and verification of an engineering database for materials for fusion power reactors. Work to date has brought SSTT to a robust state of maturity. SSTT specimens and techniques now routinely serve as the foundation for a number of ongoing and planned experimental programs. Moreover, the need to use small specimens has given rise to the development of new approaches to fracture assessment, such as the master curves-shifts method. Nonetheless a wealth of opportunities exists to further develop new and very innovative SSTT methods not only for characterizing standard mechanical properties but also to enable both large matrix single variable experiments and highly controlled basic mechanism studies. This paper reviews briefly the recent progress on developing a more science-based SSTT, including some future opportunities. The importance and utility of applying a variety of quasi-non-destructive evaluations to a single specimen and closely integrating finite element simulations and fundamental models of deformation and fracture are emphasized.
© 2002 Elsevier Science B.V. All rights reserved.

1. Introduction

Small specimen test technology (SSTT) has been an integral part of fusion materials development since the beginning. In part, this has been driven by limited availability of effective irradiation volumes in test reactors and accelerator-based neutron and charged particle sources. Consequently, a substantial effort has gone in to the development of small specimens and corresponding test techniques from which useful mechanical property information can be derived. These developments have been the subject of at least six international symposia [1–6] and several review papers [7–9]. The efforts have resulted in a substantial array of specimens with major dimensions less than a few centimeters, from which a host of mechanical properties can be derived. These include specimens that are miniaturized versions of their full-scale counterparts:

(a) tensile,
(b) low and high cycle fatigue,
(c) fracture toughness (both compact tension and bend bar geometries),
(d) fatigue crack growth,
(e) pressurized creep tubes,
(f) notched and pre-cracked impact specimens.

In addition, a variety of tests have been devised to extract mechanical properties from existing small volume specimens. For instance, the following tests have been developed for typical application to 3 mm diameter transmission electron microscopy (TEM) discs or coupon specimens:

* Corresponding author. Tel.: +1-805 893 4069; fax: +1-805 893 8124.
E-mail address: gene@engineering.ucsb.edu (G.E. Lucas).

0022-3115/02/$ - see front matter © 2002 Elsevier Science B.V. All rights reserved.
PII: S0022-3115(02)01171-6

(a) hardness and microhardness, including various elaborated and instrumented variants,
(b) ball punch,
(c) shear punch.

A subset of these specimens and test techniques have been tentatively selected as candidates for materials response verification in the international fusion materials irradiation facility, a D-Li based high energy neutron source currently undergoing conceptual design [10].

To some extent, then, SSTT has become 'mature' with a number of widely accepted test techniques and specimen geometries. In addition, a number of collateral advantages have been derived from specimens with such small dimensions. These include reduced temperature uncertainties in irradiation environments with high gamma heating; reduced dose uncertainties in the presence of significant flux gradients; more efficient use of limited amounts of material, such as experimental heats or specially doped alloys; and lower radiation dose rates and activities of irradiated materials that must be handled and ultimately disposed. Further, the success in deriving flow and fracture data from small specimens has forced a physically based consideration of ways of translating these data into the integrity assessment of large structures. Given the breadth of techniques and literature associated with SSTT, it is important to emphasize that this paper cannot present a comprehensive review or even a complete set of references.

Rather, in reviewing recent progress and new opportunities, we will focus on more recent efforts to develop a fundamental understanding of basic flow and fracture mechanisms. Achieving this objective requires close integration of experiments and models. The latter rely heavily on finite element (FE) simulations of both macroscopic test observables (e.g., loads, displacements and geometry changes) and internal distributions of stress and strain (e.g., crack tip fields). Such enhanced understanding and modeling enormously extend the information that can be derived from SSTT. Along with providing important measures of mechanical properties, small specimens greatly increase the range of irradiation and material conditions that can be explored in basic mechanism and single variable experiments. Moreover, they are consistent with developing multipurpose specimens and the design of composite specimens to address outstanding issues, such as the effect of high helium levels on fast fracture.

2. Fracture

The most recent efforts in fracture SSTT have been pursued within the framework of the master curves-shifts, MC-ΔT, method proposed by Odette and coworkers [11,12] for bcc alloys currently being considered as candidates for fusion reactor structures – namely, tempered ferritic/martensitic steels (FMS) and vanadium-based alloys. The MC-ΔT represents a significant extension and modification of recent developments in measuring cleavage initiation toughness for heavy section component integrity assessments [13]. As illustrated in Fig. 1, the shape of the effective fracture toughness K_e as a function of test temperature, T, is assumed to be described by a universal MC, or small family of curves, $K_{mc}(T - T_0)$, which is indexed by a reference temperature T_0 at a reference toughness K_r (heavy dashed curve). A relatively small number of small specimens can be used to index a baseline K_e (solid curve). Within limits, the testing conditions may deviate from small scale yielding (SSY) and the data can be adjusted to conditions of higher or lower constraint (e.g., larger or smaller dimensions) associated with size and geometry by an amount ΔT_g [14]. The position of the curve is also adjusted using additional shifts, ΔT, to account for strain rate, ΔT_{sr} (not shown) and irradiation, ΔT_i (dashed-dotted curve) as well as a margin of safety, ΔT_m (not shown). Additional shifts can also be imposed to account for statistical weakest link-type size effects [15].

Moreover, a variety of small specimens can be used to measure the shifts due to strain rate and irradiation

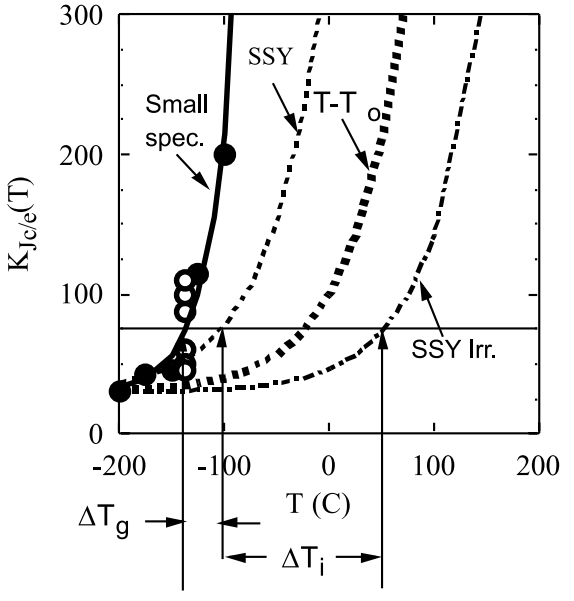

Fig. 1. Schematic illustration of the MC-ΔT method. The heavy dashed curve shows the basic MC shape on a $T - T_0$ reference scale. The solid curve represents a small specimen MC with a steeper slope and lower T_0 (referenced at 75 MPa m) by ΔT_g than the corresponding SSY curve dotted line. It has been temperature indexed with a small number of small specimens. Irradiation shifts the SSY curve by an additional increment ΔT_i, shown by the dashed-dotted line.

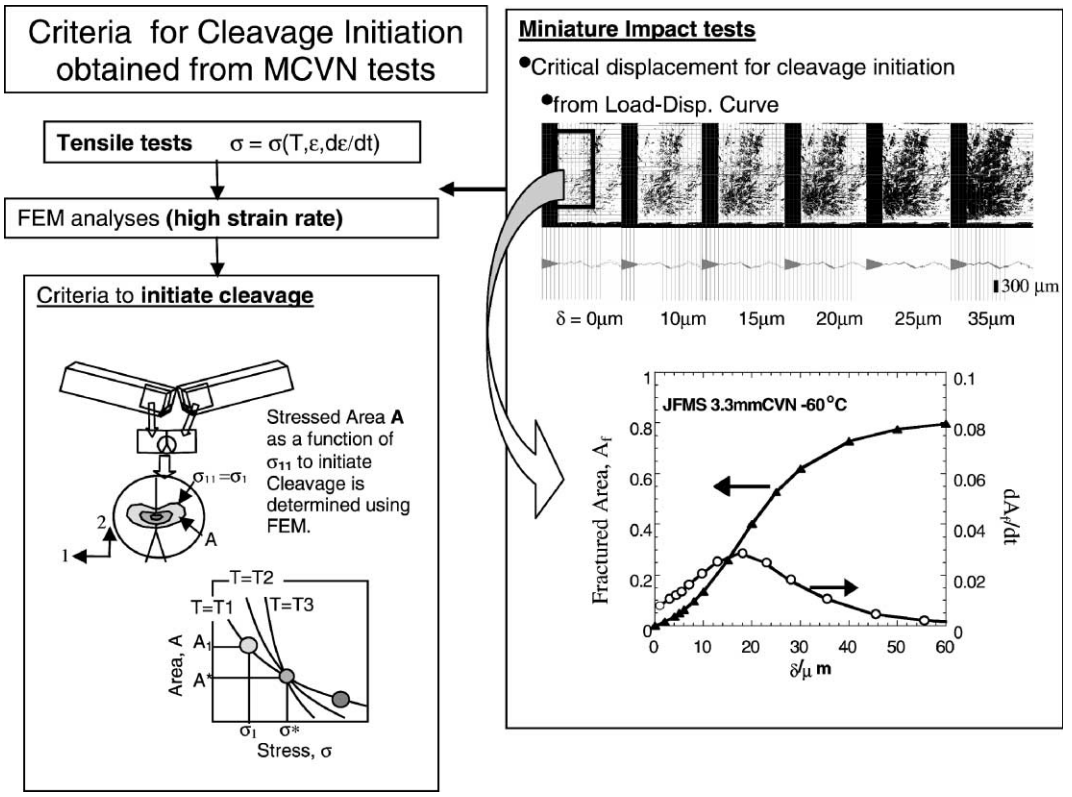

Fig. 2. Schematic illustration of integrating SSTT, confocal micrscopy/fracture reconstruction techniques and FE to obtain critical stress σ^* and critical area A^* parameters dictating the local conditions for cleavage fracture. This example is for subsized notched impact specimens.

both directly or based on mechanism based correlations [11,16]. Ultimately, microstructurally based models will be developed to predict the shifts as well as the shape and position of the reference curve [17,18].

To this end, a number of experiments are either under way or in the planning stages that involve a range of specimen sizes and crack geometries to determine values of ΔT_g in both the unirradiated and irradiated condition, along with corresponding values of ΔT_i, as well as to verify the invariance of the MC shape. For example the master curve experiments – a collaborative effort among UC Santa Barbara, CRRP (Centre de Recherches en Physique des Plasmas, Switzerland) and NRG (Nuclear Research and Consultancy Group, Petten) – focus on obtaining such data on both F82H and Eurofer97, using both the Petten high flux reactor (HFR) and the Budapest research reactor (VVRSz-M10). These experiments include a range of fracture specimen sizes, crack length to specimen width ratios, tensile specimens to obtain constitutive behavior for reasons discussed below, as well as an array of microstructural specimens.

In addition, small specimens can be used to derive micromechanically based local fracture properties, which can in turn be used in models of $K_e(T)$ and ΔT. Figs. 2 and 3 illustrate this point. Fig. 2 shows how both small fracture specimens and miniature tensile specimens can be used in conjunction with confocal microscopy/fracture reconstruction (CM/FR) techniques [19–21] to determine values of critical stress σ^* and critical area A^* within this stress contour, describing the local conditions ahead of a blunting crack at the onset of unstable cleavage crack propagation [22]. In this particular case, the specimens are subsized Charpy V-notch (CVN) impact specimens, rather than pre-cracked fracture specimens. Both specimen types provide direct local measures of effective toughness as a function of test temperature. The fracture surfaces are analyzed by CM/FR to determine the critical notch or crack tip opening δ^* corresponding to the onset of crack initiation. Miniature tensile specimens are used to obtain the materials constitutive equation, $\sigma(\varepsilon, d\varepsilon/dt, T)$, over strains, ε, strain rates, $d\varepsilon/dt$, and temperatures, T, pertinent to the deformation ahead of the crack. The constitutive law is then used in a FE analysis to simulate the deformation ahead of the notch or blunting crack tip in various specimens. The locus of the area (A) enclosed within a specified stress contour (σ) at the fracture loading conditions reflects possible combinations of A^* and σ^*. The

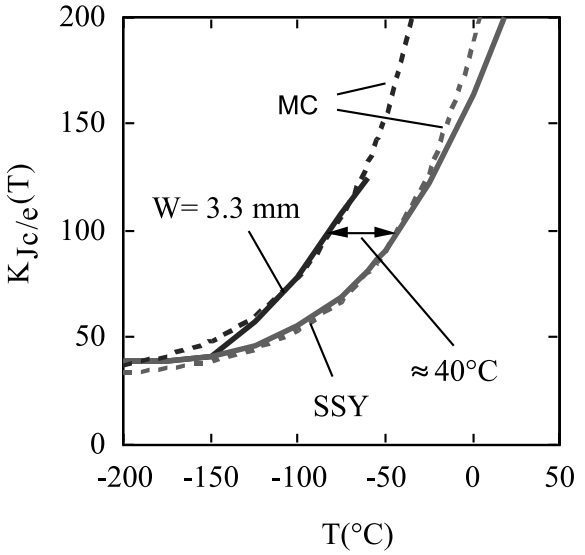

Fig. 3. Illustration of the application of $A^*(\sigma^*)$ to FE calculations of crack tip fields to determine toughness–temperature curves for both SSY conditions and subsize specimen testing. The dotted lines are MC comparisons [12].

$A(\sigma)$ corresponding to cleavage initiation are determined from these simulations at various test temperatures and for different specimens. Ideally, the $A(\sigma)$ curves intersect at a common value corresponding to $A^*(\sigma^*)$.

The inverse problem is illustrated in Fig. 3 [12]. Here the constitutive equation for an FMS has been used in an FE analysis to simulate the deformation of a fracture specimen under conditions of SSY at $K_J(T) = K_{Jc}(T)$ at the specified critical $A^*(\sigma^*)$ condition. The agreement of the predicted $K_{Jc}(T)$ curve with the MC shape is seen to be quite good. The corresponding calculated curve for a pre-cracked 1/3-sized Charpy specimen, which experiences large scale yielding, is shown for comparison. In this case, the reduced constraint in the smaller specimen leads to a downward shift in temperature of about 40 °C at a reference toughness value of $K_r = 100$ MPa m. The MC shifted down by 40 °C is also shown to be in reasonably good agreement with this smaller specimen $K_e(T)$. However, the model predicts that the smaller specimen loses its ability to undergo cleavage at a lower toughness of around 120 MPa m; and in general, the $K_e(T)$ slope in the transition region is steeper for smaller specimens [11,14].

The success in utilizing small specimens to obtain meaningful and useful fracture toughness information has led to an even more aggressive approach to reducing fracture specimen sizes. As described in a companion paper [23], recent efforts at UCSB have been successful in developing a small pre-cracked bend bar nominally 1/6 in size in all dimensions compared to a standard CVN specimen for measuring toughness at dynamic loading rates, K_{md}. The small volume of the so-called deformation and fracture minibeam (DFMB) permits a very large number of specimens to be irradiated in a small volume (e.g., nominally 216 in the volume of a standard CVN specimen). Note the small notched and un-notched DFMBs will also be used in deformation studies. Further, the actual DFMB dimensions will be adjusted for the particular material to assure that the microstructures fall within limits imposed by factors such as statistical sampling requirements and restrictions imposed by the particular application.

Fig. 4 shows recent dynamic $K_{md}(T)$ data for the IEA heat of modified F82H. A relatively sharp toughness transition occurs at a temperature $T_{md} \approx -70 \pm 10$ °C. This is significantly higher than the static $K_{Jc} = 100$ MPa m T_0 ($\approx -100 \pm 25$ °C) found with larger specimens with nominally similar material, but taken from different plates or plate sections. However, the results can be interpreted to indicate that the higher dynamic loading rate somewhat overcompensates for the reduction in the miniature specimen dynamic transition temperature (T_{md}) associated with the very small ligament size. Similar tests on a reactor pressure vessel (RPV) steel suggested that the two competing effects are approximately equal in this case.

Although the shape of the $K_e(T)$ for the DFMB specimen deviates from the MC shape, the sharper

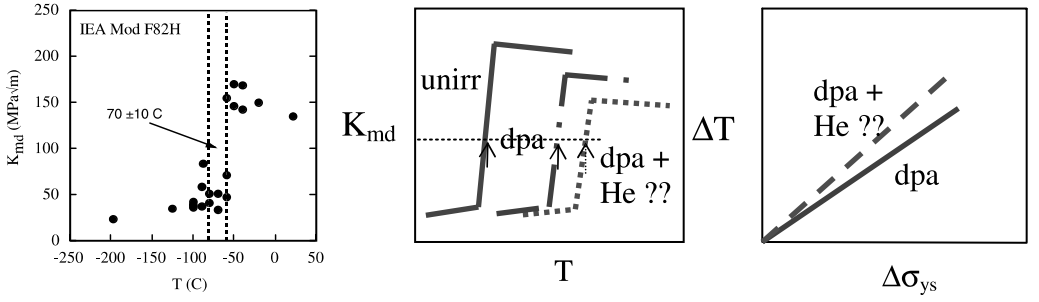

Fig. 4. (a) Illustration of $K_{md}(T)$ data obtained on 1/6-sized bend bar specimens for F82H; (b) and (c) show how such data might be applied to a determination of the effect of transmutant He on fracture behavior.

transition temperature actually facilitates the quantification of T_{md}, and hence the determination of individual contributions from multiple variables to ΔT_i – such as the possible effect of helium. This is also illustrated in Fig. 4. It is expected that DFMB type specimens will be used in an upcoming series of irradiations in the HFIR reactor as part of US–Japanese collaborations. DFMBs, with even smaller. 1×1 mm cross sections, are planned for irradiation in high energy spallation proton beams.

To date the current development of the MC-ΔT method has not included consideration of statistical weakest size effects, which is a central part of the standard ASTM MC approach [13]. A recent mechanism based analysis of a large single variable database on a RPV steel showed that both constraint loss and statistical effects are important and can be quantified based on FE simulations incorporating either deterministic or statistical micromechnical models [15,24]. Thus future research will carry out a similar evaluation of the fusion materials of prime interest and refine the MC-ΔT method to appropriately account for statistical size effects.

Before leaving the subject of fracture SSTT, it should be noted that work also continues on deriving fracture information from various kinds of punch tests. Zhang and Ardell have analyzed ball punch test parameters to suggest that fracture toughness of several ceramics could be obtained by applying analytical solutions to equations of elasticity theory [25]. Foulds et al. applied FE simulations of the ball punch process to determine critical strain energy densities for ductile failure in a number of materials, which they propose can, in turn, be used to predict fracture toughness [26]. It is also argued that the biaxial stress state in these tests is a better representation of failure conditions pertinent to fracture of cracked specimens. However, the validity of these claims depends on the situation, and biaxial results are not directly transferable to fracture under conditions of high levels of triaxial constraint.

3. Fatigue

Efforts have continued both in Germany and Japan to reduce the size scale of fatigue specimens. Based on detailed FE simulations, Moslang [27] have developed an optimized miniature fatigue specimen with a cylindrical gage section approximately 2 mm in diameter and 7.6 mm in length. The results to date indicate excellent agreement between S–N (stress amplitude, S, versus number of cycles to failure, N) data from these small specimens and much larger standard specimens. Hirose et al., have developed a similarly sized, but hourglass-shaped, specimen with commensurately good results [28]. The hourglass geometry offers the ability to achieve higher strain ranges in push-pull fatigue tests, and greater ease in temperature control. On the other hand, the strain ranges of technological interest are achievable with the cylindrical gage section; in addition, a greater volume and surface area can be tested for the same overall specimen size, and the results are more straightforward to apply in design.

There have been similar efforts to reduce the size of specimens for generating fatigue crack propagation data. For instance, Li and Stubbins have developed a bend bar that is $8 \times 4 \times 1$ mm^3 in dimension. Room temperature tests to date on an austenitic 304 stainless steel, a high-nickel Inconel 718 alloy and a modified 9Cr–1Mo steel have shown that crack growth rates da/dN versus stress intensity range ΔK data are in very good agreement with the trend curves obtained on these materials with large standard CT specimens [29]. This small specimen size, similar to a DFMB, also promises to provide opportunities to include large numbers of these specimens in irradiation experiments. Moreover, as discussed below, these specimen geometries may lend themselves to opportunities to perform multiple tests before fatigue crack growth tests are performed.

4. Deformation

Test techniques to characterize the constitutive behavior $\sigma(\varepsilon)$ of irradiated materials have continued to evolve, based on miniature tensile tests, various kinds of punch tests as well as microhardness and instrumented hardness tests.

Miniature tensile specimens for fusion materials applications have largely focused on the flat, dogbone geometry, with typical specimen gage length widths in the range 0.5 mm $\leqslant w \leqslant$ 4.5 mm and thicknesses 0.05 mm $\leqslant t \leqslant$ 1 mm [9]. The smaller dimensions are typically mediated by considerations of surface defects introduced in the fabrication process and/or grain sizes. A detailed characterization of the size limitations of miniature tensile specimens was carried out in a recent US–Japan collaboration for several austenitic and ferritic/martensitic steels. It was shown that to obtain yield stress data independent of specimen size requires specimen thickness/grain size greater than a limiting value (e.g., $t \approx 0.2$ mm for the FMS investigated). On the other hand, geometry independent ultimate tensile stress (UTS) and uniform elongation required an aspect ratio (gage thickness to width) greater than a minimum value (e.g., $\sim$0.2 for the FMS investigated) [30]. Extension of such studies to irradiated materials is an important objective.

Odette and coworkers have recently demonstrated the utility of analyzing the deformation of a tensile specimen by FE analysis [31,32]. By comparing experimental engineering stress–strain behavior to the corresponding FE

predictions, self-consistent true stress–strain constitutive equations are derived. This work demonstrated that yield drops and loss of uniform elongation in irradiated materials is a function of both irradiation hardening and loss of strain-hardening capacity. The irradiated material constitutive equations show some initial softening over a few percent strain, followed by a modest but finite strain hardening regime. Notably, significant irradiation hardening persists up to high strains. Further, the results support the use of incremental flow plasticity laws in FE studies [31,32].

Shear punch tests can be used to estimate yield strength and UTS [33,34]. In the shear punch test, a flat cylindrical penetrator is forced through a clamped coupon or disc specimen. Loads at deviation from linearity and maximum loads are used to obtain effective shear yield and ultimate stresses, which in turn empirically correlate to the corresponding uniaxial properties [33,34]. Tolozcko et al. have used FE to simulate the shear punch test with emphasis on assessing load train compliance effects. This has lead to several improvements in the test apparatus, including a shortened, stiffer penetrator, and more direct measurement of the punch displacement, resulting in improved correlation between shear punch-uniaxial tensile properties [35]. In a related series of tests, Toloczko et al. found little dependence of yield and ultimate stress on the specimen thickness (t) to grain size (d) ratio for $t/d \geqslant 5$ [36]. Gelles et al. have recently reported the use of a shear punch specimen for multipurpose applications [37]. They demonstrated that the 1 mm blank produced from a shear punch test on a 3 mm TEM specimen of irradiated steel can be inserted into an unirradiated TEM disc with a corresponding 1 mm hole, and the composite specimen jet thinned to produce an electron transparent specimen. Remnants of the irradiated ring were then used to measure the transmutant H and He concentrations. Opportunities to optimize information that can be obtained from a single specimen are discussed further below.

Changes in hardness and microhardness have long been used to track yield and tensile stress changes in irradiated materials. Moreover, instrumenting the hardness or microhardness tests has led to semi-empirical expressions that relate various features of the load-penetration data to the constitutive equation [38–40]. It has also been shown that post-test measurements of the indentation pile-up geometry can be used to estimate the strain hardening [41–45]. However, the overall effectiveness of these methods is limited. Recent FEA simulations of the ball indentation process showed that the semi-empirical relations used to predict $\sigma(\varepsilon)$ from instrumented ball indentation data are only applicable to a limited range of material behavior [46]. Constitutive equations of the following form were used in FE to simulate the ball penetration process

$$\sigma = \begin{cases} E\varepsilon & \text{for } \varepsilon \leqslant \sigma_y/E, \\ \sigma_y & \text{for } 0 < \varepsilon_p < \varepsilon_L, \\ \alpha\varepsilon_p^n & \text{for } \varepsilon_L < \varepsilon_p < \varepsilon_2, \\ \sigma_B & \text{for } \varepsilon_P > \varepsilon_2. \end{cases} \quad (1)$$

That is, the material is taken to deform elastically up to the yield stress, σ_y. Between the yield point and a strain of ε_L, the material deforms plastically at a constant stress of σ_y, simulating Luders-type strain (but distributed homogeneously). Between plastic strains ε_p of ε_L and ε_2, the material strain hardens by a degree characterized by the strain hardening exponent n. The strain level ε_2 is taken to be a saturation strain, beyond which no further hardening occurs. The simulations were carried out for combinations of: (a) two different values of the yield stress ($\sigma_y = 500$ and 792 MPa); (b) five strain hardening exponents ($n = 0.0$, 0.05, 0.1, 0.2 and 0.3); (c) four Luders strains ($\varepsilon_L = 0.002$, 0.005, 0.01 and 0.02); (d) and six levels of saturation strain ($\varepsilon_2 = 0.0625$, 0.125, 0.25, 0.5, 0.75 and 1.0). The elastic modulus E was taken to be 200 GPa (typical of steel). Load-penetrator displacement P–h_t pairs obtained from the simulations were then used with the set of semi-empirical relations that converts P–h_t pairs to σ–ε data pairs [38,40]. As one example, Fig. 5 compares the predicted σ–ε data pairs with the input constitutive equations for several representative cases. While reasonable agreement is obtained between predicted and nominal input values for values of $0.1 < n < 0.2$, the predicted data fall above and below the input constitutive equation for small n and large n, respectively. Moreover, the semi-empirical relations (by virtue of the nature of the instrumented ball indentation data) do not capture the low strain (the yield stress) and high strain (saturation stress) features of the constitutive equation.

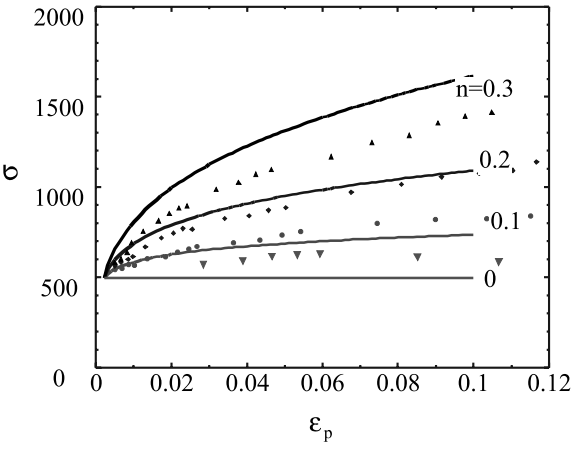

Fig. 5. Comparison of the ball indentation based estimates of σ versus ε_p (symbol points) with the input stress–strain curves (solid lines) for four constitutive laws: $\sigma_y = 500$ MPa and $n = 0$ to 0.3.

As described in a companion paper [23], insight from FE simulations of the penetration process has led to a new approach to more accurately predicting yield stress from a combined analysis of load-penetration curves and indentation pile-up geometry. This is based on FE simulations of a cone penetrator indentation with various constitutive equations similar to the type described in Eq. (1). As illustrated in Fig. 6, the aspect ratio of the indentation pile-up – that is, the pile-up height h_p to width L_{oo} ratio – correlates with the strain hardening exponent, and is only slightly sensitive to yield strength. The load (P)–penetration (Δ) curves can be fit by a parabolic function of the form

$$P = C_1\Delta_t + C_2\Delta^2. \tag{2}$$

The second derivative (curvature) of $P(\Delta)$, C_2, is sensitive to both n and σ_y. Hence, in principle, the aspect ratio gives an estimate of n, and the n and measured C_2 can be used to estimate σ_y. By iterating, a value of σ_y with decreasing uncertainty is obtained. Experimental verification of this approach is currently underway.

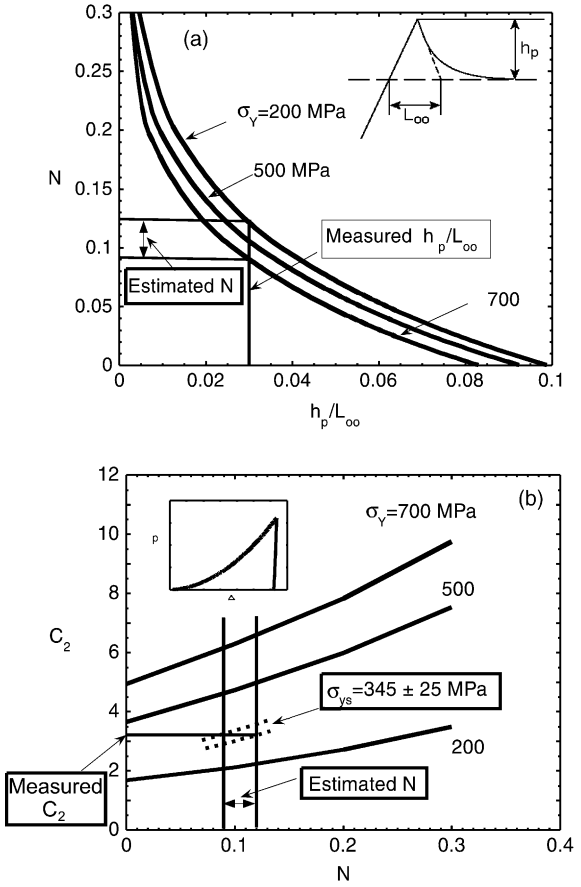

Fig. 6. Illustration of a method for combining indentation pile-up data with instrumented penetrator load-displacement curves to determine yield strength.

5. Future opportunities

The demonstrated success in applying FEA simulations to analyze and understand the flow processes involved in both uniaxial tension tests and hardness indentation tests provides a context for using other deformation tests to obtain constitutive behavior under a variety of stress-state and flow geometry conditions that are more directly pertinent to many applications than the uniaxial tensile test. Examples of these applications include triaxial stresses at crack tips, shear dominated flow geometries, high strains and deformation with internal damage evolution. Hence, it will be important to interrogate constitutive behavior under a variety of loading conditions. In addition to the tests described previously, these include: (a) bending of smooth and notched DFMBs that can be combined with microhardness traverses across the neutral axis to obtain constitutive behavior at high plastic strains, (b) bi-notched-specimen and torsion tests to characterize constitutive behavior and deformation patterns under shear dominated conditions; (c) the use of notches, dimples and holes in axially loaded coupons to locally vary the deformation stress-state [47]. The overall objective is to develop fundamental constitutive and micromechanical failure descriptions of material behavior used in FE simulations to self consistently predict the array of test results, hence, provide a reliable basis for component level deformation and fracture predictions for arbitrary stress-state and flow geometry conditions. Enriching our basic understanding of the flow and fracture of irradiated materials in this way will permit not only better structural integrity assessments but it will also enable improved designs that optimize materials performance capabilities and help guide development of improved materials systems.

As illustrated earlier, a number of attempts have been made recently to measure a series of different properties using a single specimen. With the advent of numerous new techniques that are non-destructive or semi-non-destructive in nature, the opportunity exists to significantly extend the development of multipurpose specimens. As described briefly in a companion paper [23], it is be possible to obtain mechanical property, microchemical, and microstructural and other data from small coupon-type specimens not only following irradiation but also post irradiation annealing. This involves applying a sequence of tests to the same specimen – e.g., microhardness, resistivity, Seebeck coefficient, small angle neutron scattering and positron annihilation. Ultimately, the specimens can be subject to destructive mechanical testing and/or microstructural analyses (e.g., tensile, bending and punch deformation and fracture tests, TEM, atom probe and so on). The opportunity to apply multiple techniques to a single specimen also opens the way to accelerate material development. For

instance, arrays of small specimens, systematically varied in composition and/or heat treatment can be interrogated by multiple semi-automated techniques as a means of rapidly sampling property changes as a function of a large matrix of material variables.

Finally, as discussed elsewhere [23], there are numerous opportunities to apply composite specimen based methods to interrogate limited quantities of material. For example, in principle only a few grams of ^{54}Fe can be used to produce a large number of composite fracture specimens to explore the effects of He and H on the fast fracture of FMS. In this case an embedded ^{54}Fe-based alloy is limited to the process zone at the trip of a crack by diffusion bonding it to a larger volume of normal steel to provide load transfer and appropriate stress-state constraint.

6. Conclusions

This review shows that the past development of a wide range of techniques has brought SSTT to a robust state of maturity. Tests that were considered novel a short time ago, now routinely serve as the foundation for a number of ongoing and planned experimental programs. Efforts, such as developing the MC-ΔT method, have also provided sharp focus on the challenge of using any laboratory test result to predict the in-service integrity of actual structures, and have highlighted the imperative of integrating closely these mutually dependent and complementary tasks. Nonetheless a wealth of other opportunities exists to further develop new and very innovative SSTT methods. This must be aimed not only at characterizing standard properties, but also enabling both large matrix single variable experiments and highly controlled basic mechanism studies. Future SSTT will marry a variety of quasi-non-destructive evaluations including microstructural and microchemical analysis. It has also been shown that to be effective SSTT must be closely integrated with FE simulations and fundamental models of deformation and fracture.

Acknowledgement

This work was supported in part by the US Office of Fusion Energy Sciences, grant number DE-FG03-94ER54275.

References

[1] W.R. Corwin, G.E. Lucas (Eds.), The Use of Small-Scale Specimens for Irradiated Testing, ASTM-STP-888, American Society for Testing and Materials, Philadelphia, PA, 1986.
[2] Report of the US Japan Workshop on Small Specimen Testing Techniques, Dept. Fuels Mater. Res., JAERI, 1988.
[3] P. Jung, H. Ullmaier (Eds.), Miniaturized Specimens for Testing of Irradiated Materials, Proc. IEA Symp., Jülich, 1995.
[4] IEA Symposium on Small Specimen Test Technology for Fusion Materials, Sendai, Japan, March, 1996, unpublished proceedings.
[5] W.R. Corwin, S.T. Rosinski, E. van Walle (Eds.), Small Specimen Test Techniques, ASTM-STP-1328, American Society for Testing and Material, Philadelphia, PA, 1998.
[6] M. Sokolov, G.E. Lucas, J. Landes, 4th Symposium on Small Specimen Test Techniques, ASTM-STP-1418, American Society for Testing and Material, Philadelphia, PA, in preparation.
[7] G.E. Lucas, J. Nucl. Mater. 117 (1983) 327.
[8] G.E. Lucas, Metall. Trans. 21A (1990) 1105.
[9] P. Jung, A. Hishinuma, G.E. Lucas, H. Ullmaier, J. Nucl. Mater. 232 (1996) 186.
[10] H. Matsui, IFMIF status and perspectives, presented at ICFRM-10.
[11] G.R. Odette, K. Edsinger, G.E. Lucas, E. Donahue, in: W.R. Corwin, S.T. Rosinski, E. van Walle (Eds.), Small Specimen Test Techniques, ASTM-STP-1328, American Society for Testing and Material, Philadelphia, PA, 1998, p. 298.
[12] G.R. Odette, M. He, J. Nucl. Mater. 283–287 (2000) 120.
[13] ASTM E 1921-97, Standard test method for determination of reference temperature T_0, for ferritic steels in the transition range. Annual Book of ASTM Standards 03.01, ASTM, 1998, p. 1068.
[14] G.R. Odette, M. He, C. Lee, in: M. Sokolov, G. Lucas, J. Landes (Eds.), ASTM-STP-1418, American Society for Testing and Materials, Conshohoken, PA, in preparation.
[15] H.J. Rathbun, G.R. Odette, M.Y. He, On the size scaling of cleavage toughness in the transition: a single variable experiment and model based analysis, in: International Conference (or Congress) on Fracture 10, ICF1009120R, in press.
[16] E. Donahue, G.R. Odette, G.E. Lucas, J. Nucl. Mater. 283–287 (2000) 518.
[17] G.R. Odette, G.E. Lucas, Radiat Eff. Def. Solids 144 (1998) 189.
[18] G.R. Odette, G.E. Lucas, J. Metals 53 (July) (2001) 18.
[19] K. Edsinger, PhD thesis, Department of Chemical and Nuclear Engineering, University of California, Santa Barbara, 1995.
[20] G.E. Lucas, G.R. Odette, K. Edsinger, B. Wirth, J.W. Sheckherd, in: Proceedings of the 17th Symposium on the Effects of Irradiation on Materials, ASTM-STP-1270, American Society for Testing and Materials, Philadelphia, PA, 1996, p. 790.
[21] T. Yamamoto, G.R. Odette, G.E. Lucas, H. Matsui, J. Nucl. Mater. 283–287 (2000) 992.
[22] G.R. Odette, J. Nucl. Mater. 215 (1994) 45.
[23] G.R. Odette, M. He, D. Gragg, D. Klingensmith, G.E. Lucas, Some recent innovations in small specimen testing, these Proceedings.

[24] H. Rathbun, PhD thesis, Department of Mechanical and Environmental Engineering, University of California, Santa Barbara, 2002.
[25] J. Zhang, A. Ardell, J. Mater. Res. 6 (1991) 1950.
[26] J. Foulds, P. Woytowitz, T.K. Parnell, C.W. Jewett, J. Test. Eval. 23 (1995) 3.
[27] A. Moslang, Development of creep fatigue specimen and related test technology, IFMIF User Meeting, Tokyo, Japan, 2000.
[28] T. Hirose, H. Sakasegawa, A. Kohyama, Y. Katoh, H. Tanigawa, ASTM STP 1405, American Society for Testing and Materials, Conshohoken, PA, 2001, p. 535.
[29] M. Li, J. Stubbins, in: M. Sokolov, G. Lucas, J. Landes (Eds.), ASTM-STP-1418, American Society for Testing and Materials, Conshohoken, PA, in preparation.
[30] Y. Kohno, A. Kohyama, M.L. Hamilton, T. Hirose, Y. Katoh, F.A. Garner, J. Nucl. Mater. 283–287 (2000) 1014.
[31] M. He, E. Donahue, G.R. Odette, in: M. Sokolov, G. Lucas, J. Landes (Eds.), ASTM-STP-1418, American Society for Testing and Materials, Conshohoken, PA, in preparation.
[32] G.R. Odette, M.Y. He, E.G. Donahue, P. Spätig, T. Yamamoto, Modeling the multiscale mechanics of flow localization-ductility loss in irradiation damaged bcc alloys, these Proceedings.
[33] G.E. Lucas, J.W. Sheckherd, G.R. Odette, The Use of Small-Scale Specimens for Irradiated Testing, ASTM-STP-888, American Society for Testing and Materials, Philadelphia, PA, 1986, p. 112.
[34] G.E. Lucas, J.W. Sheckherd, G.R. Odette, S. Panchanadeeswaran, J. Nucl. Mater. 122&123 (1984) 429.
[35] M. Toloczko, K. Abe, M.L. Hamilton, F.A. Garner, R. Kurtz, in: M. Sokolov, G. Lucas, J. Landes (Eds.), ASTM-STP-1418, American Society for Testing and Materials, Conshohoken, PA, in preparation.
[36] Y. Yokura, M. Toloczko, K. Abe, M.L. Hamilton, R. Kurtz, in: M. Sokolov, G. Lucas, J. Landes (Eds.), ASTM-STP-1418, American Society for Testing and Materials, Conshohoken, PA, in preparation.
[37] D. Gelles, M.L. Hamilton, R. Ermi, in: M. Sokolov, G. Lucas, J. Landes (Eds.), ASTM-STP-1418, American Society for Testing and Materials, Conshohoken, PA, in preparation.
[38] P. Au, G.E. Lucas, J.W. Sheckherd, G.R. Odette, Flow property measurements from instrumented hardness tests, in: Non-destructive Evaluation in the Nuclear Industry, ASM, Metals Park, OH, 1980, p. 597.
[39] K. Shinohara, G.E. Lucas, G.R. Odette, J. Nucl. Mater. 133&134 (1986) 326.
[40] F.M. Haggag, R.K. Nanstad, J.T. Huton, D.L. Thomas, R.L. Swain, in: A.A. Braun, N.E. Ashbaugh, F.M. Smith (Eds.), Applications of Automation Technology to Fatigue and Fracture Testing, ASTM 1092, American Society for Testing and Materials, Philadelphia, PA, 1990, p. 188.
[41] F.M. Haggag, G.E. Lucas, Metall. Trans. 14A (1983) 1607.
[42] R. Boklen, in: J. Westbrook, H. Conrad (Eds.), The Science of Hardness Testing and Its Applications, ASM, Metals Park, OH, 1973, p. 109.
[43] K. Furuya, J. Moteff, Metall. Trans. 12A (1981) 1303.
[44] M. Jayakumar, G.E. Lucas, J. Nucl. Mater. 122&123 (1984) 840.
[45] C. Santos, G.R. Odette, G.E. Lucas, T. Yamamoto, J. Nucl. Mater. 258 (1999) 452.
[46] M.Y. He, G.R. Odette, G.E. Lucasand B. Schroeter, in: M. Sokolov, G. Lucas, J. Landes (Eds.), ASTM-STP-1418, American Society for Testing and Materials, Conshohoken, PA, in preparation.
[47] S. Wimmer, V. DeGorgi, in: M. Sokolov, G. Lucas, J. Landes (Eds.), ASTM-STP-1418, American Society for Testing and Materials, Conshohoken, PA, in preparation.